

01 Oct 2009

The Effect of Glass Synthesis Route on Mechanical and Physical Properties of Resultant Glass Ionomer Cements

A. Wren


O. M. Clarkin

F. R. Laffir

C. Ohtsuki

et. al. For a complete list of authors, see https://scholarsmine.mst.edu/che_bioeng_facwork/1189

Follow this and additional works at: https://scholarsmine.mst.edu/che_bioeng_facwork

 Part of the [Biochemical and Biomolecular Engineering Commons](#), and the [Biomedical Devices and Instrumentation Commons](#)

Recommended Citation

A. Wren et al., "The Effect of Glass Synthesis Route on Mechanical and Physical Properties of Resultant Glass Ionomer Cements," *Journal of Materials Science: Materials in Medicine*, vol. 20, no. 10, pp. 1991 - 1999, Springer, Oct 2009.

The definitive version is available at <https://doi.org/10.1007/s10856-009-3781-6>



This work is licensed under a [Creative Commons Attribution 4.0 License](#).

This Article - Journal is brought to you for free and open access by Scholars' Mine. It has been accepted for inclusion in Chemical and Biochemical Engineering Faculty Research & Creative Works by an authorized administrator of Scholars' Mine. This work is protected by U. S. Copyright Law. Unauthorized use including reproduction for redistribution requires the permission of the copyright holder. For more information, please contact scholarsmine@mst.edu.

The effect of glass synthesis route on mechanical and physical properties of resultant glass ionomer cements

A. Wren · O. M. Clarkin · F. R. Laffir · C. Ohtsuki ·
I. Y. Kim · M. R. Towler

Received: 25 February 2009 / Accepted: 8 May 2009 / Published online: 21 May 2009
© Springer Science+Business Media, LLC 2009

Abstract Glass ionomer cements (GICs) have potential orthopaedic applications. Solgel processing is reported as having advantages over the traditional melt-quench route for synthesizing the glass phase of GICs, including far lower processing temperatures and higher levels of glass purity and homogeneity. This work investigates a novel glass formulation, BT 101 (0.48 SiO₂–0.36 ZnO–0.12 CaO–0.04 SrO) produced by both the melt-quench and the solgel route. The glass phase was characterised by X-ray diffraction (XRD) to determine whether the material was amorphous and differential thermal analysis (DTA) to measure the glass transition temperature (T_g). Particle size analysis (PSA) was used to determine the mean particle size and X-ray photoelectron spectroscopy (XPS) was used to investigate the structure and composition of the glass. Both glasses, the melt-quench BT 101 and the solgel BT 101, were mixed with 50 wt% polyacrylic acid (M_w , 80,800) and water to form a GIC and the working time (T_w) and the setting time (T_s) of the resultant cements were then determined. The cement based on the solgel glass had a longer T_w (78 s) as compared to the cement based on the melt derived glass (19 s). T_s was also much longer for the cement based on the solgel (1,644 s) glass than for

the cement based on the melt-derived glass (25 s). The cements based on the melt derived glass produced higher strengths in both compression (σ_c) and biaxial flexure (σ_f), where the highest strength was found to be 63 MPa in compression, at both 1 and 7 days. The differences in setting and mechanical properties can be associated to structural differences within the glass as determined by XPS which revealed the absence of Ca in the solgel system and a much greater concentration of bridging oxygens (BO) as compared to the melt-derived system.

1 Introduction

Glass ionomer cements (GICs) are used in dental applications as luting cements and as colour matched alternatives to amalgam restoratives [1]. They have potential as bone cements because of their ability to adhere to both surgical metals and the mineral phase of bone [2, 3], they set without shrinkage [4] or significant heat evolution [5] and have mechanical properties comparable to bone [6, 7]. GICs can be formulated to release clinically beneficial amounts of active ions, such as fluoride (F⁻), which can help to prevent secondary caries [8]. GICs set by the reaction of an alumino-silicate glass with an aqueous solution of polyalkenoic acid (PAA); the acid attacks and degrades the glass structure, releasing metal cations into the aqueous phase. These cations then become chelated by the carboxylate groups on the acid chains and serve to crosslink the matrix [1, 2]. The set cement consists of reacted and un-reacted glass particles embedded in a hydrated polysalt matrix. Setting is a continuous process evidenced by a change in mechanical properties with time [9].

A. Wren (✉) · O. M. Clarkin · F. R. Laffir · M. R. Towler
Clinical Materials Unit, Materials and Surface Science Institute,
University of Limerick, National Technological Park,
Limerick, Ireland
e-mail: Anthony.Wren@ul.ie
URL: www.ul.ie/ccu

M. R. Towler
e-mail: mark.towler@ul.ie

C. Ohtsuki · I. Y. Kim · M. R. Towler
Department of Crystalline Materials Science, Graduate School
of Engineering, Nagoya University, Nagoya, Japan

Unfortunately, numerous cases of aluminium induced encephalopathy have been reported [10–13] due to the release of the neurotoxic Al^{3+} ion from the mantle of set GPCs in vivo and, subsequently, aluminium based GPCs are contraindicated for use in skeletal applications, particularly for procedures where the cement could come in contact with cerebrospinal fluid (CSF) [11, 12]. The authors have previously reported the development of aluminium-free GPCs for consideration as skeletal materials [14–19]. These materials are based on predicate dental materials and exhibit similar properties to their predecessors but are formed from a calcium–strontium–zinc–silicate glass, thus eliminating the threat of aluminium induced neurotoxicity. These novel zinc based GPCs (Zn-GPCs) have strengths suitable for load bearing applications [14], demonstrable bioactivity in vivo [16], and are inherently antibacterial [15] due to the release of bacteriocidal ions (Zn^{2+} and Sr^{2+}) from the cement mantle.

The glass phase of GICs have conventionally been synthesised by the melt quench route, where the constituent oxide powders of the glass are heated together at temperatures of 1,200–1,600°C. However, there has long been interest in synthesising glasses by the solgel route as this is reported as having the potential to achieve high levels of chemical homogeneity and purity [20], and requires far lower processing temperatures than the melt quench route, meaning that the solgel process has the potential to yield glasses which cannot be easily prepared by melt quenching [21].

The solgel method is based on the formation of an inorganic network by hydrolysis and polymerisation of alkoxides in an aqueous medium and subsequent gelation [22]. Drastic changes occur at the molecular level as well as the microscopic level as the liquid is transformed to a gel, and then to the glassy state [23]. It remains unclear whether or not the glasses produced by the solgel route differ from those prepared by the melt quench method with respect to structure and physical properties [24]. Several studies have been reported on the structural differences of glasses produced by the two routes [21] and, in some cases, glasses produced by the solgel route were more homogeneous than those by the melt quench route; in line with conventional thinking [25, 26], but others have reported higher levels of heterogeneity and phase separation in the solgel glasses [27]. Few have reported how the preparation route affects the structural and mechanical properties of GICs formulated from acid degradable glasses produced by the two synthesis methods [21, 28] and none have reported on these matters when the glass in question does not contain fluoride. The glasses employed to formulate GICs in this work are both fluoride and aluminium-free and have potential as bone void fillers in the orthopaedics field. Synthesising these glasses by the melt quench route

requires very high temperatures (1,480°C), which can be difficult to maintain in a laboratory furnace. The objective of this research is to determine whether it is possible to formulate these acid degradable glasses by the solgel route and whether GICs subsequently formulated from them have markedly different physical and mechanical properties, which may be related to the homogeneity and phase purity of the mother glasses.

2 Materials and methods

2.1 Melt derived glass synthesis

A glass formulation, $4\text{SrO} \cdot 12\text{CaO} \cdot 36\text{ZnO} \cdot 48\text{SiO}_2$ (BT 101), was produced by the traditional melt quench method. Glasses were prepared by weighing out appropriate amounts of analytical grade reagents (Sigma-Aldrich, Dublin, Ireland) and ball milling (1 h). The mix was oven dried (100°C, 1 h), then fired (1,480°C, 1 h) in a mullite crucible and shock quenched into water. The resulting frit was dried, ground and sieved to retrieve a glass powder with a maximum particle size of 45 μm .

2.2 Solgel glass synthesis

BT 101 was also prepared by hydrolysis and polycondensation of tetraethoxysilane (TEOS, $\text{Si}(\text{C}_2\text{H}_5\text{O})_4$, Nacalai Tesque Inc., Japan) in strontium nitrate ($\text{Sr}(\text{NO}_3)_2$, Kishida Chemical Co. Ltd., Japan), calcium nitrate tetrahydrate ($\text{Ca}(\text{NO}_3)_2 \cdot 4\text{H}_2\text{O}$, Nacalai Tesque Inc., Japan) and zinc nitrate hexahydrate ($\text{Zn}(\text{NO}_3)_2 \cdot 6\text{H}_2\text{O}$, Nacalai Tesque Inc., Japan) in aqueous solution.

Strontium nitrate, calcium nitrate and zinc nitrate were dissolved into distilled water and nitric acid (60 wt% HNO_3 , Nacalai Tesque Inc., Japan) was subsequently added. Then TEOS was added to the above solution under stirring. After 20 min, the solution was transferred into a polystyrene square case with its top sealed tightly, and stored in an air-circulating oven for gelation and aging (40°C, 1 day). After the wet gel was dried (40°C, 7 days), it was heated (600°C, 2 h) and the residue was subsequently pulverized using a planetary ball mill.

2.3 Glass characterisation

2.3.1 X-ray diffraction (XRD)

Diffraction patterns were collected using a Philips Xpert MPD Pro 3040/60 X-ray diffraction unit (Philips, Netherlands). Disc samples (32 mm \varnothing x 3 mm) were prepared by pressing a selected glass powder (<45 μm) into a backing of ethyl cellulose (8 tons, 30 s). Samples were then placed

on spring-back stainless steel holders with a 10 mm mask and were analysed using Cu $K\alpha$ radiation. A generator voltage of 40 kV and a tube current of 35 mA was employed. Diffractograms were collected in the range $5^\circ < 2\theta < 80^\circ$, at a scan step size 0.0083° and a step time of 10 s. Any crystalline phases present were identified using JCPDS (Joint Committee for Powder Diffraction Studies) standard diffraction patterns.

2.3.2 X-ray photoelectron spectroscopy

XPS was performed in a Kratos AXIS 165 spectrometer using a monochromatic Al $K\alpha$ radiation of energy 1486.6 eV. Surface charge was efficiently neutralised by flooding the sample surface with low energy electrons. C 1s peak at 284.8 eV of adventitious carbon was used as the charge reference in determining the binding energies (B.E). Elemental analyses were obtained from a survey spectrum scanning the entire binding energy and then high resolution spectra were taken at each photoelectron transition, such as Zn 2p, O 1s, Si 2p, Sr 3p and Ca 2p with a 20 eV pass energy, 0.05 eV step size and 100 ms dwell time per step. Photoelectrons were collected at a normal take off angle relative to the sample surface. Construction and peak fitting in the narrow range spectra used a Shirley type background and the synthetic peaks were of a mixed Gaussian-Lorentzian type. The glass samples were analysed as powders.

2.3.3 Energy dispersive X-ray analysis

EDX was performed using a JOEL JSM-840 SEM (JOEL, Japan) with an accelerating voltage of 20 kV. The SEM was equipped with an energy dispersive X-ray (EDX) system (Princeton Gamma Tech EDX, New Jersey, USA) used to carry out the chemical analysis. All EDX spectra were collected at 20 kV, using a beam current of 0.26 nA.

2.3.4 Differential thermal analysis (DTA)

A combined differential thermal analyser–thermal gravimetric analyser (DTA–TGA) (Stanton Redcroft STA 1640, Rheometric Scientific, Epsom, UK) was used to measure the glass transition temperature (T_g) for both glasses. A heating rate of $10^\circ\text{C min}^{-1}$ was employed using an air atmosphere with alumina in a matched platinum crucible as a reference. Sample measurements were carried out every 6 s between 30°C and $1,000^\circ\text{C}$.

2.3.5 Particle size analysis (PSA)

Particle size analysis was achieved using a Coulter Ls 100 Fluid module particle size analyzer (Beckman Coulter, Fullerton, CA, USA). The glass powder samples were

evaluated between 0.375 and $948.2\ \mu\text{m}$ in propan-2-ol ($10\text{--}37^\circ\text{C}$), with a run length of 62 s. The relevant volume statistics were calculated on each glass.

2.4 Cement preparation

Cements were prepared by thoroughly mixing the glass powders ($<45\ \mu\text{m}$) with E9 polyacrylic acid (PAA— M_w , 80,800, $<90\ \mu\text{m}$, Advanced Healthcare Limited, Kent, UK) and distilled water on a glass plate. The cements were formulated at a P:L ratio of 2:1.5, where 1 g of BT 101 glass was mixed with 0.37 g E9 PAA and 0.37 ml water. Complete mixing was undertaken within 20 s. Both the melt quench and the solgel BT 101 were mixed with 50 wt% E9 PAA.

2.5 Determination of working and setting times

The setting times (T_s) of the cement series were tested in accordance with ISO9917; the standard for dental water based cements [29]. The working time (T_w) of the cements was measured in ambient air using a stopwatch, and was defined as the period of time from the start of mixing during which it was possible to manipulate the material without having an adverse effect on its properties.

2.6 Determination of compressive strength

The compressive strengths (σ_c) of the cements were evaluated in accordance with ISO9917 [29]. Cylindrical samples were tested after 1 and 7 days. Testing was undertaken on an Instron 4082 Universal Testing Machine (Instron Ltd., High Wycombe, Bucks, UK) using a 5 kN load cell at a crosshead speed of $1\ \text{mm/min}^{-1}$.

2.7 Determination of biaxial flexural strength

The flexural strengths (σ_f) of the cements were evaluated by a method described by Williams et al. [30]. Cement discs were tested after 1 and 7 days. Testing was undertaken on an Instron 4082 Universal Testing Machine (Instron Ltd., High Wycombe, Bucks, UK) using a 1 kN load cell at a crosshead speed of $1\ \text{mm/min}^{-1}$.

3 Results and discussion

This study determines any existing differences between the glass phase and subsequent properties of GICs formulated by two different glass production routes, the traditional melt-quench route and the solgel process. Initially, XRD was used to determine if any phase separation was induced during production of the both variants of BT 101 glass.

From Fig. 1 it can be seen that low levels of crystallinity were present in the solgel-derived BT 101.

The melt-derived BT 101, however, was amorphous. It has been suggested that glasses produced by the solgel route are more likely to induce crystallisation than their melt derived counterparts [24]. This is due to solgel glasses having a greater tendency to volume nucleation [31], which may be related to homogeneity within these glass [24]. Studies on melt-derived and solgel-derived aluminosilicate glasses of equivalent compositions showed that only surface nucleation occurred on the surface of the melt derived glass while the solgel glass showed high rates of volume nucleation [31]. It is also known that phase separation occurs in gels far below T_g , hence phase separation is achieved more readily in gels than in the corresponding melt-quench glass [24].

XPS was also performed on both glasses to determine any compositional differences that may exist between the two production routes. Table 1 presents the relative composition in the melt derived and solgel glasses as determined by quantitative XPS. It can be seen that the melt-quench route produced a glass with a higher concentration of modifying cations within the glass, particularly in the case of Zn.

It is also evident that, with the solgel route, there was no Ca present in the resulting glass. EDX (Figs. 2 and 3) was performed on samples from both the solgel and melt-quench BT 101 glass to confirm the absence of Ca from the solgel-derived glass. In both cases however, the Sr peak was masked by the Si peak.

Network modifiers, such as Ca^{2+} in this instance, play an important role in the glass where they act as a charge balancing agents [32]. The lack of Ca^{2+} will likely disrupt this process and result in the recruitment of other

Table 1 Quantitative XPS analysis of melt-derived and solgel derived BT 101 glass

	Melt derived BT 101 (% at conc)	Solgel derived BT 101 (% at conc)
Zn 2p	7.0	1.7
Sr 3p	1.5	1.3
Ca 2p	2.5	0
Si 2p	29.5	37.4
O 1s	46.2	53.4
C 1s	13.3	6.2

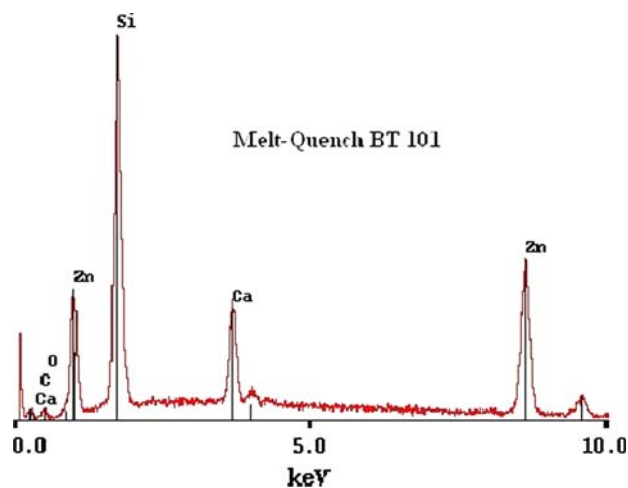
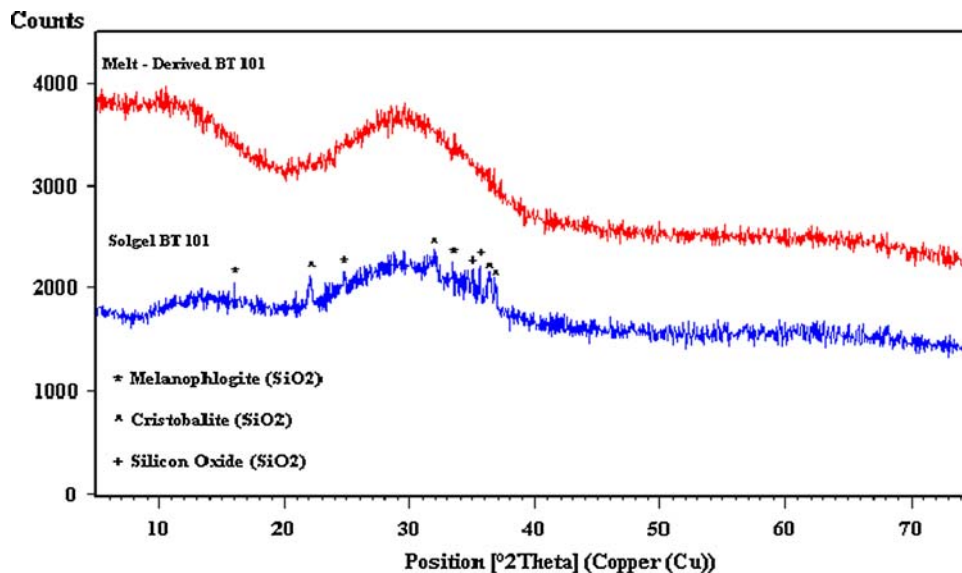


Fig. 2 EDX spectra of melt quench BT 101 glass

modifying cations, in this case Zn^{2+} or Sr^{2+} , to replace Ca^{2+} . Sr^{2+} and Ca^{2+} share atomic similarities, i.e. their atomic radii (Ca—0.94 nm, Sr—1.16 nm) [33]. The lack of Ca will subsequently result in a lower concentration of modifying cations in the solgel-derived BT 101 glass

Fig. 1 XRD of melt-quench and solgel BT 101 glasses



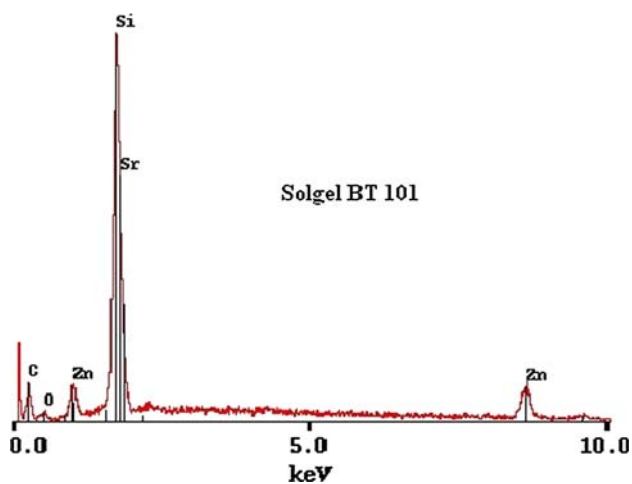


Fig. 3 EDX spectra of solgel BT 101 glass

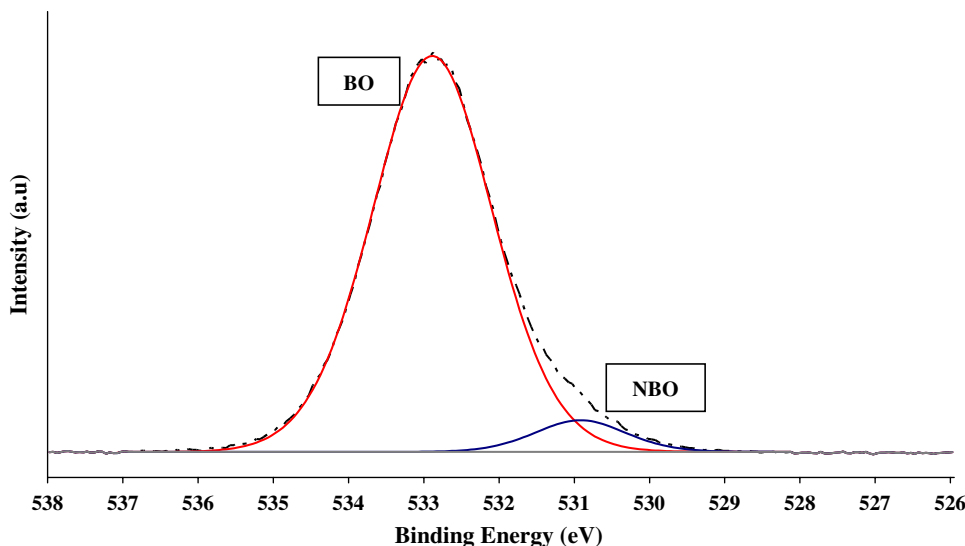
Table 2 Cation to Si ratio for melt-derived and solgel-derived BT 101

	Cation (% at conc)	Si (% at conc)
Melt	1	2.7
Solgel	1	12.5

structure. From Table 1, the cation to Si ratio was calculated and is presented in Table 2.

It is evident that there is a much higher concentration of Si in relation to the cation concentration with the solgel-derived BT 101. This is likely due to the absence of Ca in the glass, resulting in Sr adopting its role in the glass network. It is also evident that the Zn concentration is lower in the solgel-derived glass as compared to the melt derived glass. This reduced concentration of modifiers will also contribute to lowering the amount of non-bridging oxygen (NBO) species in the solgel-derived glass.

Fig. 4 O1s photoelectron spectrum of solgel BT 101 glass



XPS is sensitive to changes in the local chemical environment of atoms which results in chemical shifts in the binding energy. High resolution O 1s spectra for the solgel-derived and the melt-derived glasses are shown in Figs. 4 and 5, respectively. Deconvolution of the O 1s spectrum in Fig. 4 gives a well resolved peak at 532.9 eV associated with Si–O–Si units (bridging oxygen groups (BO)) [24]. The accompanying shoulder at lower binding energy (531 eV) can be attributed to non bridging oxygen (NBO) where one of the Si atoms is replaced by a modifying cation. The O 1s spectrum of melt derived glass (Fig. 5) is not resolved; however, it is apparent that two peaks are necessary to describe it. By constraining the peak width (FWHM) of the higher binding energy (BO) component to that of O 1s in Fig. 4 on the assumption that these arise from chemically similar environments, the peak can be fitted as shown in Fig. 5. The two component peaks at 532.3 eV and 531.1 eV can be assigned to BO and NBO respectively. The resulting ratio of BO:NBO in the two glass samples are markedly different with the melt derived glass having a higher proportion of NBO. In Table 2, modifier cation concentration to Si is compared and shows that melt derived glass has nearly five times more modifiers than the solgel derived glass. Increased concentration of modifier cations facilitates the replacement of bridging oxygen with non-bridging oxygen groups within the silica network. Hence a higher proportion of NBO is expected and observed in the melt derived glass. Similar to the O 1s spectra, shift in the Si 2p peak to lower binding energy ($\Delta E = 1$ eV) is observed in the melt derived sample which has a lower Si content (a higher cation content). It is evident from Figs. 4 and 5 that there is a higher concentration of NBOs to BOs in the melt-derived system as compared to the solgel-derived glass.

Fig. 5 O1s photoelectron spectrum of melt quench BT 101 glass

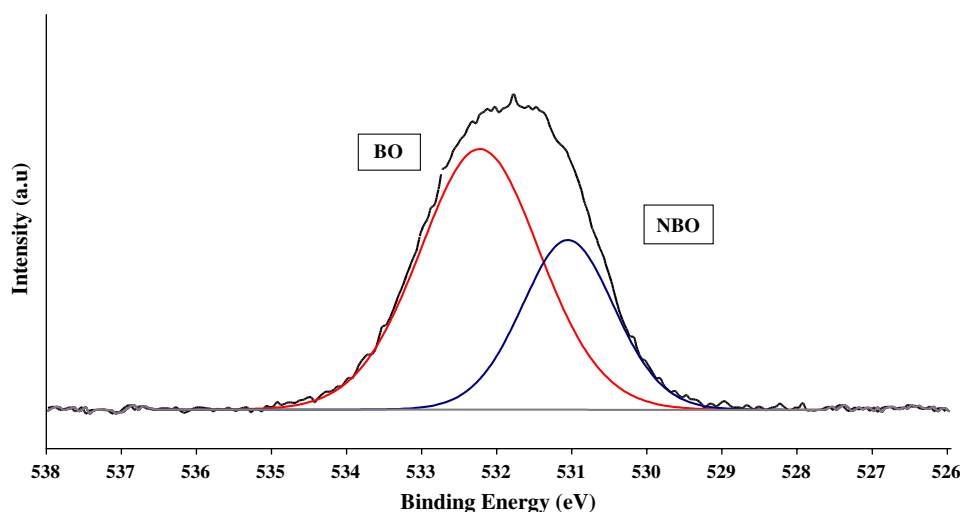
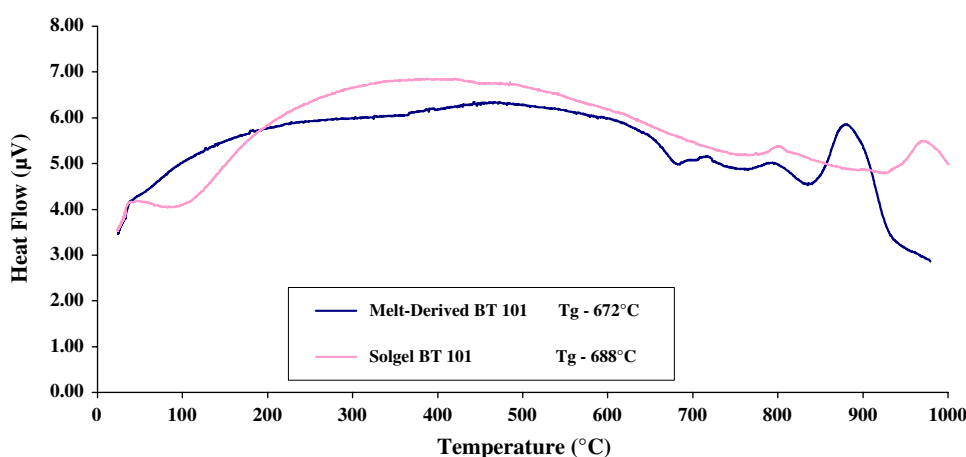


Fig. 6 DTA of melt-quench and solgel BT 101 glasses



The binding energies of the two components are close to those reported by Roy et al. [23, 24] in their study of alkali silicate glasses prepared from solgel and melt quench methods ($\text{Na}_2\text{O-SiO}_2$ and $\text{Li}_2\text{-SiO}_2$). This study found that by heating the solgel glass, more NBO were formed and the structure evolved towards the melt-derived glass network. This was attributed to increasing temperature (300–500°C) where heat treatment of the gel promoted de-polymerisation [24]. The formation of more NBOs indicates that more alkali cations are breaking the Si–O–Si network upon heating [24]. However in the case of the solgel glass under investigation here it is likely that the maximum number of NBOs have been formed since the glass was heat treated close to T_g . This may be due to the ratio of network modifier to silica concentration in the glass considering the two different glass production routes, where lower concentration of modifier in the solgel-derived glass inhibits its ability to reach similar levels of NBO species compared to melt derived glass.

The thermal properties of the glass were investigated using differential thermal analysis and are presented in Fig. 6.

The glass transition temperature (T_g) for the melt-derived BT 101 glass was found to be 672°C, while the solgel-derived BT 101 glass was found to be 688°C. The higher T_g in the solgel glass may be due to a reduced rate of reactivity as compared to the melt-derived glass. This may be due to the higher concentration of BO in the solgel-derived glass which induces a more stable glass network [32]. The higher concentration of cations in the melt-derived system may lead to ionic bonding between alkali cation and the NBO [23] which subsequently requires less energy to reach T_g . The first crystallisation temperatures (T_{c1}) for both glasses were found to be similar, (melt-derived, 796°C and solgel-derived, 803°C), however the second crystallisation temperature (T_{c2}) was considerably higher in the solgel glass, (976°C, as compared to 887°C). This may also be due to the glass structure where the solgel-derived glass may require more energy to form complex crystalline structures.

Particle size analysis was also performed on both glasses and the results are presented in Table 3.

The solgel-derived glass was found to have a greater overall particle size distribution ($d_{<50\%} = 10.05 \mu\text{m}$) as

Table 3 Particle size analysis results

	$d_{<10\%}$	$d_{<50\%}$	$d_{<90\%}$
Solgel BT 101 (m)	2.12	10.05	48.13
Melt derived BT 101 (m)	1.18	5.63	14.13

compared to the melt derived glass ($d_{<50\%} = 5.63 \mu\text{m}$). A smaller glass particle size increases exposed surface area, thereby producing greater dissolution during the setting reaction [34]. However, this increase in exposed surface area is also known to facilitate a decrease in the working (T_w) and setting time (T_s). In this study, cements formulated from the solgel glass exhibited a longer T_w and considerably longer T_s than those formulated from the melt derived glass (Fig. 7).

T_w was determined as being 78 s for a GIC formulated from the solgel-derived glass and 19 s for one formulated from melt-derived glass. T_s of GIC based on the melt-derived glass was 25 s while that of a GIC based on solgel-derived glass was 1644 s. The explanation for the extended

T_w , and particularly T_s , is related to structural differences within the glass, rather than particle size effects. As already determined by XPS, the solgel-derived glass contains a significantly lower concentration of NBOs as compared to the melt-derived glass. This reduced concentration of NBOs lowers the rate of silica dissolution and hence the glasses ability to degrade and form a crosslinked network during setting [35]. The high concentration of NBOs in the melt-derived system results in a glass that is more susceptible to acid attack which facilitates a more rapid setting reaction. Choi et al. [36] influenced the bioactivity of a GIC by adding solgel glass ($\text{CaO-P}_2\text{O}_5\text{-SiO}_2$) to a commercial Fuji I (GC, Japan). They found that by increasing the solgel concentration, hardening was retarded. This was attributed to reduced cationic release rate as compared to the glass phase of the commercial GIC [36]. This also suggests that the solgel route produces glasses with a reduced ionic dissolution rate as compared to the traditional melt-quench method.

Mechanical testing was also undertaken on cements formulated from glasses containing both the melt-quench

Fig. 7 Working and setting times of GICs formulated from melt quench and solgel BT 101 glasses

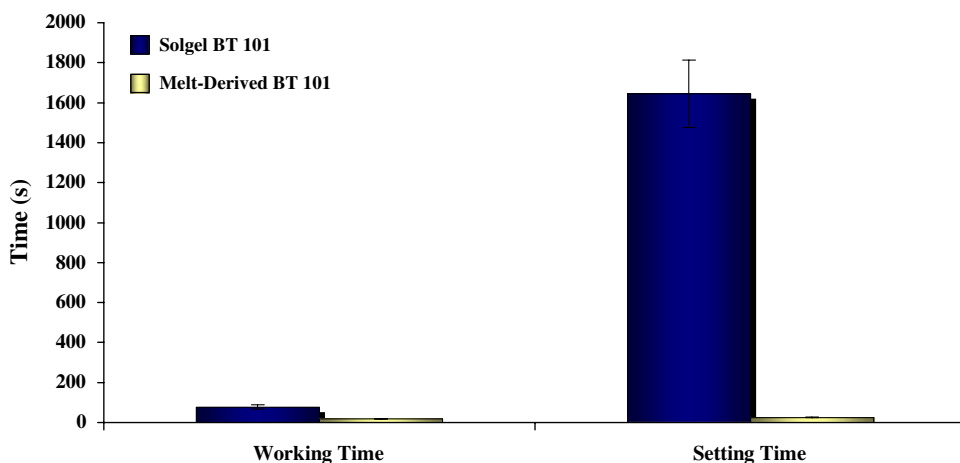


Fig. 8 Compressive strengths of GICs formulated from melt quench and solgel BT 101 glasses after 1 and 7 day maturation

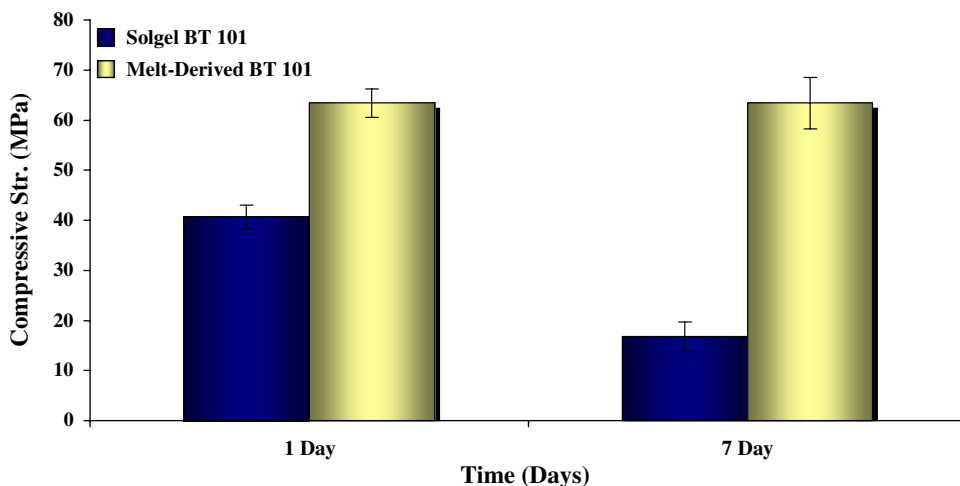
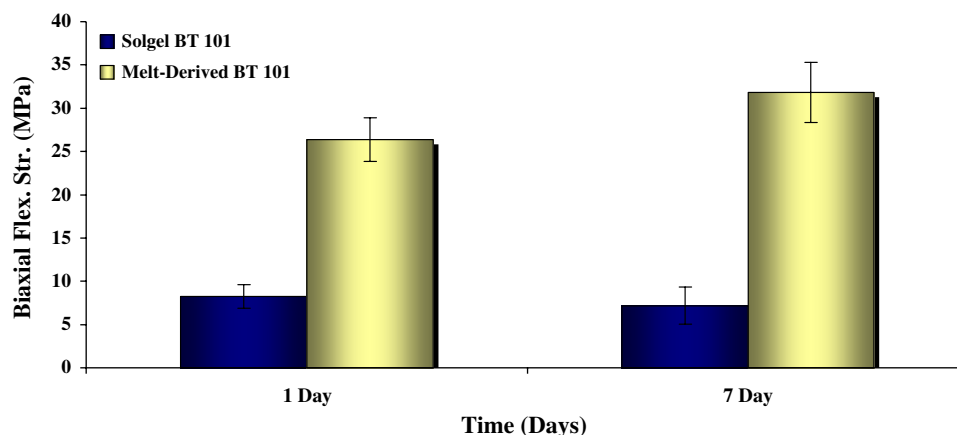


Fig. 9 Biaxial flexural strengths of GICs formulated from melt quench and solgel BT 101 glasses after 1 and 7 day maturation



and solgel route. Compressive (σ_c) testing and biaxial flexural (σ_f) testing were performed over 1 and 7 days.

The σ_c of cements synthesised from the melt-derived glass (Fig. 8) remained relatively constant with respect to maturation (63 MPa), while the solgel-derived glass produced cements that significantly reduced in strength over time (40 MPa at 1 day, 16 MPa at 7 days). This may be attributed to test modality as the compressive test is a less discriminatory test than the biaxial flexural test, as GICs fracture at the atomic level by tensile or shear failure [37, 38]. σ_f provides a greater description of tensile strength [39]. The flexural strength of both sets of cements (Fig. 9) did not significantly change with respect to maturation. However, glasses formulated via the solgel route produced cements that were significantly weaker than those made from the melt-quench route. This is likely related to the reactivity of the glass particles. XPS determined that a greater concentration of NBOs exist in the melt-derived glass which facilitates a degradable glass network. This is required for glass particle dissolution and cross-linking of the cations and COO^- groups to occur during the setting reaction [40, 41]. The solgel-derived glass however contained a greater concentration of BOs which are impervious to acid attack and will hinder cement formation. Fracture in GICs is modelled by reptation theory, where fracture of the cement occurs due to polymer chains being displaced from their location within the cement matrix [40, 42]. The mechanical strength of GICs is determined in part by the composition of the glass phase and the molecular weight of the PAA. However, in this study, the glass composition, molecular weight and concentration of the polyacid used to formulate the cements were the same. Therefore it is the concentration of bridged COO^- groups that determines the strength of the material, where in this case, the melt-derived glass provided a greater crosslink density within the cement matrix. This is due to a more acid-reactive glass resulting in a greater concentration of cations available for the setting reaction.

4 Conclusions

A novel glass formulation, BT 101 (0.48 SiO_2 –0.36 ZnO –0.12 CaO –0.04 SrO) was produced by both a melt-quench and a solgel processing route. The glass produced by the solgel route had a higher T_g , which may be due to the higher concentration of bridging oxygens in the solgel-derived glass, inducing a more stable glass network.

Both the melt-quench and the solgel BT 101 glasses were mixed with 50 wt% polyacrylic acid (M_w , 80,800) and water to form a GIC. The cement based on the solgel glass had longer working and setting times (78 s and 1644 s, respectively) than the cement based on the melt derived glass (19 s and 25 s, respectively).

The cements based on the melt derived glass produced higher strengths in both compression and biaxial flexure.

The differences in setting and mechanical properties can be associated to structural differences within the glass, as determined by XPS, which revealed the absence of Ca (resulting in a lower concentration of modifying cations) and a much greater concentration of bridging oxygens in the solgel system as compared to the melt-derived system.

Acknowledgements The financial assistance of both Enterprise Ireland (TD/2005/327) and PRTL1 4 are gratefully acknowledged.

References

- Nicholson JW. Chemistry of glass-ionomer cements: a review. *Biomaterials*. 1998;19:485–94. doi:10.1016/S0142-9612(97)00128-2.
- Akinmade AO, Nicholson JW. Glass-ionomer cements as adhesives. Part I. Fundamental aspects and their clinical relevance. *J Mater Sci Mater Med*. 1993;4:93–101.
- Wilson AD, Prosser HJ, Powis DM. Mechanism of adhesion of polyelectrolyte cements to hydroxyapatite. *J Dent Res*. 1983;62:590–2.
- McLean JW. Glass ionomer cements. *Br Dent J*. 1988;164:293–300. doi:10.1038/sj.bdj.4806434.

5. Brook IM, Hatton PV. Glass ionomers: bioactive implant materials. *Biomaterials*. 1998;19:565–71. doi:10.1016/S0142-9612(98)00138-0.
6. Hatton PV, Hurrell-Gillingham K, Brook IM. Biocompatibility of glass ionomer bone cements. *J Dent*. 2006;34:598–601. doi:10.1016/j.jdent.2004.10.027.
7. Boyd D, Towler MR, Wren AW, Clarkin OM. Comparison of an experimental bone cement with surgical Simplex p, Spineplex and Cortoss. *J Mater Sci Mater Med*. 2008;19:953–7. doi:10.1007/s10856-006-0060-7.
8. Nicholson JW, Braybrook JH, Wasson EA. The biocompatibility of glass-poly(alkenoate) glass-ionomer cements: a review. *J Biomater Sci Polym Ed*. 1991;2:277–85. doi:10.1163/156856291X00179.
9. Williams JA, Billington RW. Increase in compressive strength of glass ionomer restorative materials with respect to time: a guide to their suitability for use in posterior primary dentition. *J Oral Rehabil*. 1989;16:475–9. doi:10.1111/j.1365-2842.1989.tb01368.x.
10. Hantson P, Mahieu P, Gersdorff M, Sindic CJM, Lauwerys R. Encephalopathy with seizures after use of aluminium-containing bone cement. *Lancet*. 1994;344:1634–47. doi:10.1016/S0140-6736(94)90446-4.
11. Hoang-Xuan K, Perrotte P, Dubas F, Philippon J, Poisson FM. Myoclonic encephalopathy after exposure to aluminium. *Lancet*. 1996;347:910–1. doi:10.1016/S0140-6736(96)91399-9.
12. Reusche E, Pilz P, Oberascher G, Linder B, Egensperger R, Gloeckner K, et al. Subacute fatal aluminium encephalopathy after reconstructive otoneurosurgery: a case report. *Hum Pathol*. 2001;32:1136–9. doi:10.1053/hupa.2001.28251.
13. Reusche E, Rohwer J, Forth W, Helms J, Geyer G. Ionomeric cement and aluminium encephalopathy. *Lancet*. 1995;345:1633–4. doi:10.1016/S0140-6736(95)90138-8.
14. Boyd D, Clarkin OM, Wren AW, Towler MR. Zinc-based glass polyalkenoate cements with improved setting times and mechanical properties. *Acta Biomater*. 2008;4:425–31. doi:10.1016/j.actbio.2007.07.010.
15. Boyd D, Li H, Tanner DA, Towler MR, Wall JG. The antibacterial effects of zinc ion migration from zinc-based glass polyalkenoate cements. *J Mater Sci Mater Med*. 2006;17:489–94. doi:10.1007/s10856-006-8930-6.
16. Boyd D, Towler MR. The processing, mechanical properties and bioactivity of zinc based glass ionomer cements. *J Mater Sci Mater Med*. 2005;16:843–50. doi:10.1007/s10856-005-3578-1.
17. Boyd D, Towler MR, Law RV, Hill R. An investigation into the structure and reactivity of calcium-zinc-silicate ionomer glasses using MAS-NMR spectroscopy. *J Mater Sci Mater Med*. 2006;17:397–402. doi:10.1007/s10856-006-8465-x.
18. Towler MR, Kenny S, Boyd D, Pembroke T, Buggy M, Guida A, et al. Calcium and zinc ion release from polyalkenoate cements formed from zinc oxide/apatite mixtures. *J Mater Sci Mater Med*. 2006;17:835–9. doi:10.1007/s10856-006-9843-0.
19. Towler MR, Kenny S, Boyd D, Pembroke T, Buggy M, Hill RG. Zinc ion release from novel hard tissue biomaterials. *Biomed Mater Eng*. 2004;14:565–72.
20. Hench LL, West JK. The sol-gel process. *Chem Rev*. 1990;90:33–72. doi:10.1021/cr00099a003.
21. Bertolini MJ, Zaghete MA, Gimenes R, Padovani GC. Determination of the properties of an experimental glass polyalkenoate cement prepared from niobium silicate powder containing fluoride. *Dent Mater*. 2008;24:124–8. doi:10.1016/j.dental.2007.03.005.
22. Taira M, Yamaki M. Preparation of SiO₂-Al₂O₃ glass powders by the sol-gel process for dental applications. *J Mater Sci Mater Med*. 1995;6:197–200. doi:10.1007/BF00146855.
23. Roy B, Jain H, Saha SK, Chakravorty D. Comparison of structure of alkali silicate glasses prepared by sol-gel and melt-quench methods. *J Non-Cryst Solids*. 1995;183:268–76. doi:10.1016/0022-3093(94)00633-4.
24. Roy B, Jain H, Saha SK, Chakravorty D. Phase separation and structural differences between alkali silicate glasses prepared by the sol-gel and melt-quench methods. *J Am Ceram Soc*. 1995;81:2360–70.
25. Roy R. Gel route to homogeneous glass preparation. *J Am Ceram Soc*. 1969;52:344. doi:10.1111/j.1151-2916.1969.tb11945.x.
26. McCarthy GJ, Roy R. Gel route to homogeneous glass preparation II: gelling and desiccation. *J Am Ceram Soc*. 1971;54:539. doi:10.1111/j.1151-2916.1971.tb12202.x.
27. Weinberg MC, Neilson GF. Phase separation behaviour of a metal organic derived sodium silicate glass. *J Mater Sci*. 1978;13:1206. doi:10.1007/BF00544726.
28. Bertolini MJ, Zaghete MA, Gimenes R. Development of an experimental glass ionomer cement containing niobium and fluoride. *J Non-Cryst Solids*. 2005;351:3884–7. doi:10.1016/j.jnoncrsol.2005.10.008.
29. International Organization for Standardization 9917. Dental water based cements (E). Case postale 56. Geneva, Switzerland. 1991; CH-11211.
30. Williams JA, Billington RW, Pearson GJ. The effect of the disc support system on biaxial tensile strength of a glass ionomer cement. *Dent Mater*. 2002;18:376–9. doi:10.1016/S0109-5641(01)00053-7.
31. James PF, Iqbal Y, Jais US, Jordery S, Lee WE. Characterisation of silicate and phosphate glasses. *J Non-Cryst Solids*. 1997;219:17–29. doi:10.1016/S0022-3093(97)00247-0.
32. Nicholson JW, Wilson AD. Acid-Base cements—their biomedical and industrial applications. *Chemistry of solid state materials*. Vol. 3. Cambridge; 1993.
33. Hill RG, Stamboulis A, Law RV, Clifford A, Towler MR, Crowley C. The influence of strontium substitution in fluorapatite glasses and glass-ceramics. *J Non-Cryst Solids*. 2004;336:223–9. doi:10.1016/j.jnoncrsol.2004.02.005.
34. Prentice LH, Tyas MJ, Burrow MF. The effect of particle size distribution on an experimental glass ionomer cement. *Dent Mater*. 2005;21:505–10. doi:10.1016/j.dental.2004.07.016.
35. Serra J, Gonzalez P, Liste S, Chiussi S, Leon B, Perez-amor M, et al. Influence of the non-bridging oxygen groups on the bioactivity of silicate glasses. *J Mater Sci Mater Med*. 2002;13:1221–5. doi:10.1023/A:1021174912802.
36. Choi J-Y, Lee H-Y, Kim H-E. Bioactive sol-gel glass added ionomer cement for the regeneration of the structure. *J Mater Sci Mater Med*. 2008;19:3287–94. doi:10.1007/s10856-008-3464-8.
37. Xie D, Brantley WA, Culbertson BM, Wang G. Mechanical properties and microstructures of glass ionomer cements. *Dent Mater*. 2000;16:129–38. doi:10.1016/S0109-5641(99)00093-7.
38. Prosser HJ, Powis DR, Wilson AD. Glass ionomer cements of improved flexural strength. *J Dent Res*. 1986;65:146–8.
39. Higgs WAJ, Lucksanasombool P, Higgs RJED, Swain MV. Evaluating acrylic and glass-ionomer cement strength using the biaxial flexure test. *Biomaterials*. 2001;22:1583–90. doi:10.1016/S0142-9612(00)00324-0.
40. Fennell B, Hill RG. The influence of poly(acrylic) acid molar mass and concentration on the properties of polyalkenoate cements. *J Mater Sci*. 2001;36:5193–202. doi:10.1023/A:1012445928805.
41. Cho S-Y, Cheng AC. A review of glass ionomer restorations in the primary dentition. *J Can Dent Assoc*. 1999;65:491–5.
42. Wilson AD, Hill RG, Warrens CP, Lewis BG. The influence of polyacid molecular weight on some properties of glass ionomer cements. *J Dent Res*. 1989;68:89–94.